

# Advances in Cement Research

## Advances in clinkering technology of calcium sulfoaluminate cement

--Manuscript Draft--

<b>Manuscript Number:</b>	ACR-D-17-00028R2	
<b>Full Title:</b>	Advances in clinkering technology of calcium sulfoaluminate cement	
<b>Article Type:</b>	General paper	
<b>Corresponding Author:</b>	Isabel Galan, Dr. University of Aberdeen Aberdeen, UNITED KINGDOM	
<b>Corresponding Author Secondary Information:</b>		
<b>Corresponding Author's Institution:</b>	University of Aberdeen	
<b>Corresponding Author's Secondary Institution:</b>		
<b>First Author:</b>	Isabel Galan, PhD	
<b>First Author Secondary Information:</b>		
<b>Order of Authors:</b>	Isabel Galan, PhD	
	Ammar Elhoweris	
	Theodore Hanein, PhD	
	Marcus N Bannerman, PhD	
	Fredrik P Glasser, Prof.	
<b>Order of Authors Secondary Information:</b>		
<b>Abstract:</b>	<p>A new method for producing calcium sulfoaluminate (C\$A) clinkers is described. Sulfur is introduced from the gas phase as SO<sub>2</sub> and oxygen and reacts with solids during clinkerisation. Laboratory experiments and thermodynamic calculations are presented. Sulfur-containing phases, ye'elimite and ternesite, are stabilised together with belite to produce clinkers with various mineralogies. The influence of temperature and SO<sub>2</sub> partial pressure is analysed and their effect on the formation of undesirable anhydrite and gehlenite is explained. The process by which a potentially hazardous waste material such as sulfur is used as raw material, and possibly as fuel, to form C\$A cements, is shown to be successful.</p>	
<b>Funding Information:</b>	Gulf Organisation for Research and Development (GORD) (ENG016RGG11757)	Not applicable

1  
2  
3  
4  
5  
6  
7  
8  
9  
10  
11  
12  
13  
14  
15  
16  
17  
18  
19  
20  
21  
22  
23  
24  
25  
26  
27  
28  
29  
30  
31  
32  
33  
34  
35  
36  
37  
38  
39  
40  
41  
42  
43  
44  
45  
46  
47  
48  
49  
50  
51  
52  
53  
54  
55  
56  
57  
58  
59  
60  
61  
62  
63  
64  
65

Dear editor,

According to your comments, better quality images have now been added and the format of the manuscript has been revised.

1  
2  
3 **Advances in clinkering technology of calcium sulfoaluminate cement**  
4

5 Isabel Galan, PhD

6 (corresponding author)

7 Department of Chemistry, University of Aberdeen, Aberdeen AB24 3UE, United Kingdom

8 Institute for Applied Geosciences, Graz University of Technology, Graz 8010, Austria

9 ORCID 0000-0001-6845-471X

10 igalangarcia@tugraz.at

11 Tel: +43 3168736885  
12

13 Ammar Elhoweris

14 Department of Chemistry, University of Aberdeen, Aberdeen AB24 3UE, United Kingdom

15 Gulf Organisation for research and Development, Qatar Science and Technology Park, Doha,

16 Qatar  
17

18 Theodore Hanein, PhD

19 School of Engineering, University of Aberdeen, Aberdeen AB24 3UE, United Kingdom

20 Department of Materials Science and Engineering, University of Sheffield, Sheffield S1 3JD,

21 United Kingdom  
22

23 Marcus N. Bannerman, PhD

24 School of Engineering, University of Aberdeen, Aberdeen AB24 3UE, United Kingdom  
25

26 Fredrik P. Glasser, Prof

27 Department of Chemistry, University of Aberdeen, Aberdeen AB24 3UE, United Kingdom  
28  
29  
30

31  
32 Number of words in the main text (excluding abstract and references): 5182  
33

34 Number of figures: 7  
35

36 Number of tables: 8  
37  
38  
39  
40  
41  
42  
43  
44  
45  
46  
47  
48  
49  
50  
51  
52  
53  
54  
55  
56  
57  
58  
59  
60  
61  
62  
63  
64  
65

1  
2  
3  
4  
5  
6  
7  
8  
9  
10  
11  
12  
13  
14  
15  
16  
17  
18  
19  
20  
21  
22  
23  
24

## Abstract

A new method for producing calcium sulfoaluminate ( $C\bar{S}A$ ) clinkers is described. Sulfur is introduced from the gas phase as  $SO_2$  and oxygen and reacts with solids during clinkerisation. Laboratory experiments and thermodynamic calculations are presented. Sulfur-containing phases, ye'elimite and ternesite, are stabilised together with belite to produce clinkers with various mineralogies. The influence of temperature and  $SO_2$  partial pressure is analysed and their effect on the formation of undesirable anhydrite and gehlenite is explained. The process by which a potentially hazardous waste material such as sulfur is used as raw material, and possibly as fuel, to form  $C\bar{S}A$  cements, is shown to be successful.

## Keywords chosen from ICE Publishing list

Clinkering/clinkering reactions; Diffraction (X-ray); Mineralogy; Modelling; Special cements; Thermodynamics; Waste valorisation

## List of notation

25  
26  
27  
28  
29  
30  
31  
32  
33  
34  
35  
36  
37  
38  
39  
40  
41  
42  
43  
44  
45  
46  
47  
48  
49  
50  
51  
52  
53  
54  
55  
56  
57  
58  
59  
60  
61  
62  
63  
64  
65

$C$	$CaO$
$S$	$SiO_2$
$A$	$Al_2O_3$
$\bar{S}$	$SO_3$
$F$	$Fe_2O_3$

1 **1. Introduction**

2 The formulation of calcium sulfoaluminate ( $C\bar{S}A$ ) cements is undergoing rapid development as a  
3 prelude to widespread application. The advantages of  $C\bar{S}A$  cements relative to ordinary Portland  
4 cement (OPC) have been reported (Gartner 2004, Hanein et al. 2016, Gartner, Hirao 2015,  
5 Gartner, MacPhee 2011, Juenger et al. 2011) and include reduction of  $CO_2$  emissions and lower  
6 specific energy requirements.

7 The major benefits of  $C\bar{S}A$  cements primarily arise due to the presence of abundant ye'elite  
8 ( $C_4A_3\bar{S}$ ) giving, among other advantages, high early strength. But other sulfur containing phases,  
9 including ternesite ( $C_5S_2\bar{S}$ ) and anhydrite ( $C\bar{S}$ ) can occur.  $C\bar{S}A$  clinkers require a source of sulfur  
10 trioxide, commonly provided by addition of anhydrite to the clinker or either active anhydrite or  
11 gypsum to the raw mix. However, the formation of  $C\bar{S}A$  clinker is challenging, particularly under  
12 laboratory conditions, due to volatilisation of  $SO_3$  (the stable gas phase lost at elevated  
13 temperatures is in fact a mixture of  $SO_2$  and  $O_2$  from the solids) or, more generally, the inability  
14 to stabilise the clinker  $SO_3$  content.

15 At clinkering temperatures, typically  $>1250\text{ }^\circ C$  but lower than melting temperatures, which occur  
16 at  $>1300\text{ }^\circ C$  (Idrissi et al. 2010, Touzo, Scrivener & Glasser 2013), the loss of  $SO_3$  limits  
17 clinkering to a rather narrow window of temperatures and requires that the exhaust gas from the  
18 kiln is monitored and, if necessary, scrubbed to remove  $SO_x$ . The present paper shows that this  
19 loss need not be a problem, particularly on an industrial scale: the high pressures of sulfur  
20 oxides can be used to an advantage and vapour transport is shown to be an effective way of  
21 achieving reaction amongst the components of the raw meal. Kinetic studies show that the  
22 equilibrium between gas and solid components is achieved rapidly at  $\approx 1300\text{ }^\circ C$ , even in the  
23 rapid flow rates achieved in commercial kilns.

24 Most experience of clinkering has been gained by laboratory experiments supplemented by pilot  
25 plant "burns". In the present study, a somewhat different approach was taken. Experiments and  
26 thermodynamic calculations were combined to elucidate the clinkering process. The work  
27 demonstrates the importance of the vapour phase to clinkering and has led to changes in kiln  
28 operation: the kiln is modified to work as a semi-sealed system in order to gain control of the kiln  
29 atmosphere. This has been paralleled by using a small capacity (10-100g) laboratory kiln

1 30 permitting independent control of temperature and gas partial pressures of SO<sub>2</sub> and O<sub>2</sub> and total  
2 31 pressure 1 bar.  
3  
4 32 Numerous high temperature thermodynamic equilibrium models based on Gibbs energy  
5  
6 33 minimization have been developed for cement clinker predictions and have proved useful in  
7  
8 34 cement research (Barry, Glasser 2000, Hökfors et al. 2015, Hökfors, Eriksson & Viggh 2014).  
9  
10 35 Thermodynamic databases used to calculate high temperature cement phase equilibria include,  
11  
12 36 MTDATA (Davies et al. 2002), FactSage (Bale et al. 2002), HSC (Roine 2002) and that recently  
13  
14 37 developed by Hanein et al. (Hanein, Glasser & Bannerman 2015). As shown by Hanein et al.  
15  
16 38 (Hanein et al. 2015), the stability of ye'elimite at clinkering temperatures is dependent on the  
17  
18 39 fugacities (which we equate with partial pressures) of both SO<sub>2</sub> and O<sub>2</sub> in the kiln atmosphere  
19  
20 40 and a thermodynamic model considering both the clinker phases and atmosphere has been  
21  
22 41 developed to model the reaction path and optimising operating conditions for the production of  
23  
24 42 C<sub>3</sub>A clinkers.  
25  
26  
27 43

## 28 44 **2. Experimental**

### 29 45 **2.1. Furnace**

30  
31  
32 46 Experiments were conducted in a tube furnace specifically modified to operate at one bar total  
33  
34 47 pressure but with controlled partial pressures of SO<sub>2</sub> and O<sub>2</sub> (Galan et al. 2014), see Figure 1.  
35  
36 48 The pre-mixed gases, whose rates were monitored by means of precision mass flow controllers  
37  
38 49 (Bronkhorst, NL), pass through the non-rotating furnace tube maintaining the desired  
39  
40 50 atmosphere during the experiment. The discharge end of the tube is connected to a scrubber  
41  
42 51 that absorbs and neutralizes unreacted SO<sub>x</sub> prior to gas discharge to the atmosphere. In that  
43  
44 52 way, exit gases achieve less than 1ppm SO<sub>x</sub>. Temperature patterns (heating, idling and cooling)  
45  
46 53 were programmed at the furnace control box.  
47  
48  
49 54

### 50 55 **2.2. Raw materials**

51  
52 56 Two sets of raw materials were used for the experiments:  
53  
54 57 Set 1: laboratory grades of Al<sub>2</sub>O<sub>3</sub> (Sigma-Aldrich 265497, 10 μm, 99.7%), SiO<sub>2</sub> (quartz, Fluka  
55  
56 58 83340, >230 mesh, >95%), CaCO<sub>3</sub> (Sigma-Aldrich 795445, >99%), Fe<sub>2</sub>O<sub>3</sub> (Fisher Scientific  
57  
58 59 I/1150/53, general purpose grade) and CaSO<sub>4</sub> (Fisher C/2440/60, >95%).  
59  
60  
61  
62  
63  
64  
65

1 60 Set 2: commercially available bauxite, clay and limestone. The oxide composition of the  
2 61 commercially available raw materials is shown in Table 1. The bauxite and the clay were  
3  
4 62 provided by Zhengzhou Haixu abrasives Co. Ltd. (China), and the limestone was provided by  
5  
6 63 Samin (France).

7  
8 64 In both cases the raw materials were weighted, mixed, placed in crucibles or boats of aluminous  
9  
10 65 porcelain or Pt, and introduced in the furnace which was ramped up to an isothermal level.

11  
12 66

### 13 14 67 **2.3. Experiments**

15  
16 68 The variables evaluated in the experiments described in this work include: SO<sub>2</sub> partial pressure,  
17  
18 69 peak clinkering temperature, proportioning of raw materials and time. The O<sub>2</sub> partial pressure  
19  
20 70 was kept sufficiently high to ensure oxidizing conditions to (i) prevent formation of undesirable  
21  
22 71 sulfides and (ii) ensure all SO<sub>2</sub> is able to oxidize to SO<sub>3</sub> if the equilibrium sought demands  
23  
24 72 formation of solids containing sulfate. The minimum O<sub>2</sub> excess was targeted at 100%, resulting  
25  
26 73 in weight ratios SO<sub>2</sub>:O<sub>2</sub> at least 1:0.5 (or SO<sub>2</sub>:air, 1:2.5).

27  
28 74 Approximately 25 compositions were tested and in all cases the atmosphere conditions were  
29  
30 75 such that SO<sub>3</sub> was transferred from the vapour to the solid to achieve the target mineralogy.

31  
32 76 This was achieved providing an automatic check that the kinetics of transfer of sulfur species  
33  
34 77 from gas to solid are rapid. The experiments included: (i) formation of CaSO<sub>4</sub> by transfer of  
35  
36 78 SO<sub>2</sub>+O<sub>2</sub> from the vapour to powdered CaCO<sub>3</sub> or CaO, (ii) formation of ye'elimite (C<sub>4</sub>A<sub>3</sub>S̄) and  
37  
38 79 ternesite (C<sub>5</sub>S<sub>2</sub>S̄) by transfer of SO<sub>2</sub>+O<sub>2</sub> to appropriate mixes of CaO and Al<sub>2</sub>O<sub>3</sub>, and CaO and  
39  
40 80 SiO<sub>2</sub>, respectively, and (iii) clinkers designed to contain C<sub>4</sub>A<sub>3</sub>S̄, belite (C<sub>2</sub>S) and ferrite (solid  
41  
42 81 solution C<sub>2</sub>F-C<sub>6</sub>A<sub>2</sub>F) by transfer of SO<sub>2</sub>+O<sub>2</sub> to mixes of CaO, Al<sub>2</sub>O<sub>3</sub>, SiO<sub>2</sub> and Fe<sub>2</sub>O<sub>3</sub>. The  
43  
44 82 different compositions were prepared by hand mixing the calculated amounts of dry solid  
45  
46 83 reactants using a mortar and a pestle with a few drops of ethanol added to aid homogenisation,  
47  
48 84 for 5 minutes. The resulting mix was dried in an oven at ≈100 °C for 2 hours to remove the  
49  
50 85 alcohol. Clinkers were prepared from lab grade materials in the form of pellets (Table 2) and in  
51  
52 86 powder (Table 3) and using commercially available raw materials (Table 4) in powder form with  
53  
54 87 a particle size of approximately 40 microns. In experiments 1-11 in Table 3 lab grade calcium  
55  
56 88 sulfate (C<sub>5</sub>S̄) was also added to the raw mix.

57  
58  
59 89  
60  
61  
62  
63  
64  
65

1 90 - Clinkers made with CaCO<sub>3</sub>, SiO<sub>2</sub>, Al<sub>2</sub>O<sub>3</sub> and Fe<sub>2</sub>O<sub>3</sub>. Three different mixes were  
2 91 prepared in the form of 13 mm diameter pressed pellets. These were fired at 1300 °C  
3  
4 92 for 30 minutes. Targeted mineralogies and gas flow conditions are shown in Table 2.  
5  
6 93 The amount of sulfur introduced in the furnace was in all cases sufficient to form the  
7  
8 94 target amount of C<sub>4</sub>A<sub>3</sub> $\bar{S}$ . The rate of SO<sub>2</sub> used allowed for the formation of a minimum of  
9  
10 95 1.5 grams of “SO<sub>3</sub>” in the 30 minutes the gases were passing through the tube furnace.  
11  
12 96 The quantities of SO<sub>3</sub> required to obtain the target compositions 1, 2 and 3 in Table 2  
13  
14 97 were 0.21, 0.13 and 0.05 grams, respectively. C<sub>6</sub>A<sub>2</sub>F was chosen as the target  
15  
16 98 stoichiometry for ferrite based on trends shown by Touzo et al. (Touzo, Scrivener &  
17  
18 99 Glasser 2013) for feeds with high Al<sub>2</sub>O<sub>3</sub>:Fe<sub>2</sub>O<sub>3</sub> ratios, but changes were made in the  
19  
20 100 course of the work because experiments showed that the actual ferrite lay close to  
21  
22 101 C<sub>4</sub>AF.  
23  
24 102  
25  
26 103 - Clinkers made with CaCO<sub>3</sub>, SiO<sub>2</sub>, Al<sub>2</sub>O<sub>3</sub>, Fe<sub>2</sub>O<sub>3</sub> and CaSO<sub>4</sub>. In this set of experiments  
27  
28 104 the SO<sub>2</sub>+O<sub>2</sub> was turned on when the furnace reached ≈600 °C during ramp up (at 20  
29  
30 105 °C/min) and turned off during the cooling cycle (at 20 °C/min) below ≈600 °C. To  
31  
32 106 facilitate reaction between gas and solid phases, a layer of the solid reactants several  
33  
34 107 mm thick, ≈10 grams in total, was placed in a 15 cm long ceramic boat in the middle of  
35  
36 108 the hot zone of the tube (at constant temperature). The mix proportions used and the  
37  
38 109 experimental conditions (SO<sub>2</sub>:air ratios and temperature) are summarised in Table 3.  
39  
40 110 The time allowed for reaction, ≈120 minutes, does not include ramping up and down  
41  
42 111 times. The amount of CaSO<sub>4</sub> was in all cases enough to form the desired target  
43  
44 112 compositions; the SO<sub>2</sub>+O<sub>2</sub> atmosphere was used to preclude sulfur losses from the  
45  
46 113 solids, and to keep an atmosphere with an excess of “SO<sub>3</sub>” at all times.  
47  
48 114  
49  
50 115 - Clinkers made with commercially available raw materials. Two different mixes were  
51  
52 116 used under two different conditions. The mixes used were calculated for a certain target  
53  
54 117 composition assuming silica (from both the clay and bauxite) will form belite (C<sub>2</sub>S), the  
55  
56 118 iron oxide will combine with Ca and Al oxides to form ferrite (C<sub>4</sub>AF) and the excess of Al  
57  
58 119 oxide react to form ye’elimite (C<sub>4</sub>A<sub>3</sub> $\bar{S}$ ). The gas atmosphere was on from the beginning  
59  
60  
61  
62  
63  
64  
65



1 120 to the end of the experiments (to prevent possible sulfur losses during ramping up and  
2 121 down). As in the lab grade experiments, a layer of the solid reactants several mm thick,  
3  
4 122 ≈10 grams in total, was placed in a ceramic boat in the middle of the hot zone of the  
5  
6 123 tube (at constant temperature). The proportions used and the experimental conditions  
7  
8 124 (SO<sub>2</sub> partial pressure, temperature and time) are summarised in Table 4. In the column  
9  
10 125 'time' the number indicates the actual time at peak temperature. The excess of SO<sub>3</sub> in  
11  
12 126 these cases was higher: the mass of SO<sub>3</sub> that would pass through the tube during the  
13  
14 127 time at peak temperature (around 6 g) was 3-4 times higher than the amount needed in  
15  
16 128 theory for the target mineralogies (around 2.2 g and 1.4 g, respectively). For these  
17  
18 129 experiments C<sub>4</sub>AF was chosen as the target stoichiometry for ferrite, as opposed to the  
19  
20 130 C<sub>6</sub>A<sub>2</sub>F used for the previous ones. This was done for several reasons: the exact  
21  
22 131 stoichiometry for ferrite in C<sub>3</sub>A mixes is not well known and both extremes of the solid  
23  
24 132 solution had to be checked; also, according to the results, the ferrite phase made in  
25  
26 133 SO<sub>2</sub>+O<sub>2</sub> atmospheres seems to be variable, but both the standard used for Rietveld  
27  
28 134 refinement and the data for the thermodynamic modelling consider C<sub>4</sub>AF.  
29  
30

31 135

#### 32 136 **2.4. Characterisation**

33  
34  
35 137 The products obtained were characterised by X-ray powder diffraction using an Empyrean  
36  
37 138 diffractometer (PANalytical) with strictly monochromatic CuKα1 radiation ( $\lambda = 1.54056 \text{ \AA}$ ) at 45  
38  
39 139 kV and 40 mA. In order to determine the composition of the samples, they were analysed using  
40  
41 140 the Rietveld methodology as implemented in the GSAS software package (Larson, Von Dreele  
42  
43 141 2004). Final global optimised parameters included background coefficients, zero-shift error, cell  
44  
45 142 parameters and peak shape parameters. Peak shapes were fitted using the pseudo-Voigt  
46  
47 143 function (Thompson, Cox & Hastings 1987) with an asymmetry correction included (Finger, Cox  
48  
49 144 & Jephcoat 1994). A March-Dollase ellipsoidal preferred orientation correction algorithm  
50  
51 145 (Dollase 1986) was used when preferred orientation parameter needed refinement. The crystal  
52  
53 146 structure descriptions for the different phases encountered were: (Cuesta et al. 2013) for  
54  
55 147 orthorhombic ye'elimite, (Cuesta et al. 2014) for cubic ye'elimite, (Mumme et al. 1995) for  $\beta$ -  
56  
57 148 belite, (Colville, Geller 1971) for ferrite, (Louisnathan 1971) for gehlenite, (Irran, Tillmanns &  
58  
59  
60  
61  
62  
63  
64  
65

1 149 Hentschel 1997) for ternesite, (Hörkner, Müller-Buschbaum 1976) for calcium monoaluminate,  
2 150 (Kirfel, Will 1980) for anhydrite and (Sasaki et al. 1987) for perovskite.

3  
4 151

## 5 6 152 **2.5. Thermodynamic modelling**

7  
8 153 A thermodynamic model based on Gibbs energy minimisation and a recently compiled high  
9 154 temperature cement clinker stoichiometric phase thermodynamic database (Hanein, Glasser &  
10 155 Bannerman 2015) was used to supplement the experimental data: raw mix input and  
11 156 experimental conditions included in Table 4 were 'replicated' for the model calculations. The  
12 157 thermodynamic data for ye'elimite and ternesite ( $C_5S_2\bar{S}$ ) were recently derived by the authors  
13 158 (Hanein et al. 2015, Hanein et al. 2017). The thermodynamic model and compiled database  
14 159 used here have been validated in several studies (Hanein, Glasser & Bannerman 2015, Hanein  
15 160 et al. 2015, Hanein et al. 2017, Galan et al. 2017, Hanein et al. 2016). As a means of emulating  
16 161 the furnace operation (continuous counter-current flow) and to maintain constant  $SO_2$  and  $O_2$   
17 162 partial pressures in the system, the gaseous atmosphere is assumed to be in excess ( $m_{gas} \gg$   
18 163  $m_{solids}$ ).  $P_2O_5$  and MnO were neglected in thermodynamic simulations due to the lack of  
19 164 thermodynamic data for these species and phases containing them. The database also does  
20 165 not have thermodynamic data for  $C_6A_2F$ ;  $C_4AF$  is the only calcium aluminoferrite for which data  
21 166 are currently available. The model used takes into account both the solids and the atmosphere  
22 167 surrounding them simultaneously. For comparison, only major phases formed and detected in  
23 168 XRD measurements of experimental runs are shown from the model results in Table 8.  
24 169 However, the model also accounts for all the species shown in Table 1 (except MnO and  $P_2O_5$ )  
25 170 and all the calculations carried out predict the conversion of all alkali to alkali sulfates; MgO also  
26 171 appears to remain unreacted in the thermodynamic calculations.

27  
28  
29  
30  
31  
32  
33  
34  
35  
36  
37  
38  
39  
40  
41  
42  
43  
44  
45  
46  
47 172

## 48 49 173 **3. Results**

### 50 51 174 **3.1. Transfer of sulfur between gas and solids**

52 175 The transfer of sulfur from gas to solid was confirmed to be rapid at 900-1000 °C and above:  
53 176 CaO reacted readily and completely with mixes of  $SO_2$  and  $O_2$  to form  $CaSO_4$ . For these  
54 177 experiments different flow rates and ratios  $SO_2$ :air were used (0.1:0.25, 0.434:1.058,  
55 178 0.868:2.116 and 0.217:0.529 g/min), and they were performed using different amounts of CaO

179 in powder and in porous pellets (13 mm diameter) for different periods of time (from 5 minutes to  
180 4 hours). Formation of  $\text{CaSO}_4$  was assessed quantitatively by XRD.

181

### 182 **3.2. Formation of ye'elimite, $\text{C}_4\text{A}_3\bar{\text{S}}$**

183 At  $\approx 1200\text{-}1300$  °C,  $\text{C}_4\text{A}_3\bar{\text{S}}$  was formed in  $\text{SO}_2+\text{O}_2$  atmospheres from 30 g mixes of  $\text{CaCO}_3$  and  
184  $\text{Al}_2\text{O}_3$ . Figure 2 shows the XRD pattern following 30 minutes reaction at 1220 °C, where the  
185 rates of  $\text{SO}_2$  and air used were 0.105 and 0.2624 g/min, respectively, giving a  $\text{SO}_2$ :air ratio of  
186 1:2.5. Such a high  $\text{SO}_2$  concentration did not lead to high yields of ye'elimite:  $\text{CaSO}_4$  forms,  
187 leaving unreacted  $\text{Al}_2\text{O}_3$  and  $\text{CaO}$  coexisting with  $\text{CA}_2$  and  $\text{CA}$ . The results cannot be in  
188 equilibrium as some phases are known to be incompatible, e.g.  $\text{CaO}$  and  $\text{CA}_2$  (Galan et al.  
189 2017). Re-introducing the sample for another 30 minutes in the furnace under the same  
190 conditions led to an increase in ye'elimite and a decrease in  $\text{CaSO}_4$ , leaving traces of  $\text{CA}_2$  and  
191  $\text{Al}_2\text{O}_3$  still present. Further repetition of the same process led to total disappearance of  $\text{CaO}$  and  
192  $\text{Al}_2\text{O}_3$  and some increase both in the ye'elimite yield and reduction in the  $\text{CaSO}_4$  with almost  
193 constant  $\text{CA}_2$ . After 7x30 minutes cycles, the XRD pattern did not change and it was considered  
194 that the sample reached its final state.

195 Rates of  $\text{SO}_2$  and air of 0.0525 and 1.3122 g/min, respectively (ratio  $\text{SO}_2$ :air of 1:25) were used  
196 for tests of 60 minutes duration. Figure 3 shows the result of this synthesis, performed using the  
197 same amount of raw materials (stoichiometric amounts of  $\text{CaCO}_3$  and  $\text{Al}_2\text{O}_3$  to form  $\text{C}_4\text{A}_3\bar{\text{S}}$ ) and  
198 same temperature (1220 °C) as the previous ones, for 60 minutes. As it can be seen, lower  $\text{SO}_2$   
199 partial pressure (10 times dilution) led to higher yields of  $\text{C}_4\text{A}_3\bar{\text{S}}$ , no unreacted raw materials and  
200 only small amounts of  $\text{CaSO}_4$  and  $\text{CA}$  remaining. These experiments suggest the existence of a  
201 threshold in the  $\text{SO}_2$  concentration which, if exceeded, favours reaction of  $\text{SO}_3$  with lime to give  
202  $\text{CaSO}_4$ , inhibiting formation of ye'elimite.

203

### 204 **3.3. Formation of ternesite, $\text{C}_5\text{S}_2\bar{\text{S}}$**

205 In a similar fashion to the methods used in section 4.2, the formation of  $\text{C}_5\text{S}_2\bar{\text{S}}$  was investigated.  
206 A mix of  $\text{CaCO}_3$  and  $\text{SiO}_2$  (quartz) was prepared and placed in a boat and reacted at 1220°C for  
207 60 minutes. As with the  $\text{C}_4\text{A}_3\bar{\text{S}}$  experiments, the reactive sulfur containing atmosphere was left  
208 running for the duration of the experiment. Flow-rates of 0.25 g/min air and 0.1 g/min  $\text{SO}_2$  were

1 209 used in the initial high SO<sub>2</sub> partial pressure experiment to give a ratio SO<sub>2</sub>:air 1:2.5. Figure 4  
2 210 shows that the experiment did not form ternesite and instead produced a mixture of belite,  
3  
4 211 anhydrite and unreacted material. The temperature, reaction time and cooling rates of the  
5  
6 212 reaction were altered in attempts to form ternesite but, at this partial pressure, these  
7  
8 213 experiments proved unsuccessful.  
9  
10 214 As calculation suggested that the SO<sub>2</sub> partial pressure was too high, another experiment was  
11  
12 215 conducted, where the partial pressure of the SO<sub>2</sub> component of the atmosphere was lowered,  
13  
14 216 similar to what was done in section 4.2: flow-rates of 0.1 g/min SO<sub>2</sub> and 2.5 g/min air were used  
15  
16 217 to give a ratio air:SO<sub>2</sub> of 25:1. As shown in Figure 5, ternesite was successfully formed at 1075  
17  
18 218 °C in the sulfur containing atmosphere for the first time, in the presence of belite, anhydrite and  
19  
20 219 unreacted lime. The temperature was chosen based on previous work (Pliego-Cuervo, Glasser  
21  
22 220 1978), who synthesized ternesite in sealed systems using belite and calcium sulfate as  
23  
24 221 reactants. These experiments show the combined influence of temperature and SO<sub>2</sub> partial  
25  
26 222 pressure on the stability of sulfur-containing phases. The field of stability of ternesite has  
27  
28 223 subsequently been mapped by Hanein et al. (Hanein et al. 2017) who show quantitatively the  
29  
30 224 necessity of controlling the partial pressures of gas species if ternesite is the desired product.  
31  
32  
33

225

### 226 **3.4. Synthesis of clinkers using laboratory grade reactants**

36 227 At 1300 °C clinkers containing ye'elimite, belite and anhydrite were synthesized from mixes of  
37  
38 228 CaCO<sub>3</sub>, SiO<sub>2</sub>, Al<sub>2</sub>O<sub>3</sub> and Fe<sub>2</sub>O<sub>3</sub> using both mixes of reactants in powder form and by pressing  
39  
40 229 these same mixes in the form of 13 mm diameter pellets. The thickness of the pellets was ≈ 2  
41  
42 230 mm. Three different mixes were used in order to obtain different proportions of the phases in the  
43  
44 231 final product. Targeted compositions are given in Table 2. Figure 6 and Figure 7 show the  
45  
46 232 pellets corresponding to target compositions 1 and 2, respectively. In both cases the pellets  
47  
48 233 were coherent and did not show cracking. However, the pellets with target composition 3, high  
49  
50 234 in silica, crumbled during cooling and only powder could be retrieved.

51 235 The results from Rietveld refinement of the XRD patterns of the pellets are shown in Table 5.

52 236 Mixes 1 and 2 led to formation of mainly four phases: ye'elimite, belite, anhydrite and gehlenite  
53  
54 237 (C<sub>2</sub>AS). In both cases, crystalline ferrite was almost absent. The presence of undesired C $\bar{S}$  and  
55  
56  
57  
58  
59  
60  
61  
62  
63  
64  
65

1 238 C<sub>2</sub>AS can be attributed to kinetic effects but also to the SO<sub>2</sub> partial pressure used which may  
2 239 have favoured their formation.  
3  
4 240 Mix 3 gave very different mineralogy: in this case, both β-C<sub>2</sub>S and γ-C<sub>2</sub>S were present, as well  
5  
6 241 as ferrite and tricalcium aluminate. CaSO<sub>4</sub> was absent and C<sub>4</sub>A<sub>3</sub> $\bar{S}$  and C<sub>2</sub>AS only appeared in  
7  
8 242 very low percentages. The physical decomposition of pellets, termed 'dusting', is attributed to  
9  
10 243 the volume expansion arising from spontaneous conversion of the high temperature belite  
11  
12 244 phases to γ-C<sub>2</sub>S in the course of cooling.  
13  
14 245 Table 6 shows the results obtained from Rietveld analysis for the clinkers synthesized using lab  
15  
16 246 grade reactants including CaSO<sub>4</sub> (conditions shown in Table 3).  
17  
18 247 At a constant temperature of 1280 °C, a drastic effect is observed when diluting the SO<sub>2</sub> from  
19  
20 248 SO<sub>2</sub>:air ratio of 1:2.5 to 1:25 (reactions 1 and 2, respectively, in Table 6), not only in the  
21  
22 249 formation of ye'elimite but also on the belite. High concentrations of SO<sub>2</sub> shifted the equilibrium  
23  
24 250 away from belite to mixtures of C $\bar{S}$  and C<sub>2</sub>AS. Further reduction of the SO<sub>2</sub> partial pressure  
25  
26 251 (ratios SO<sub>2</sub>:air 1:50 and 1:100 in reactions 3 and 4 in Table 6) did not lead to significant  
27  
28 252 changes in the final compositions. The remaining % of C<sub>2</sub>AS and C $\bar{S}$  are attributed to kinetic  
29  
30 253 effects: once C<sub>2</sub>AS and C $\bar{S}$  formed in quantity, 120 minutes does not seem to be sufficient to  
31  
32 254 completely shift compositions towards C<sub>2</sub>S and C<sub>4</sub>A<sub>3</sub> $\bar{S}$ .  
33  
34 255 Lower temperatures also have an impact in the final compositions, especially at the lower SO<sub>2</sub>  
35  
36 256 partial pressure conditions (experiment 5 in Table 6) at 1230 °C and 1:50 SO<sub>2</sub>:air ratio), making  
37  
38 257 it even more difficult to reach the target compositions by reacting C $\bar{S}$  and C<sub>2</sub>AS.  
39  
40 258 The effect of the gas flow rate is also shown in experiments 2 and 9. Similar temperature (1280  
41  
42 259 and 1270 °C, respectively) and partial pressure (SO<sub>2</sub>:air ratio 1:25) but different gas flow rate  
43  
44 260 (SO<sub>2</sub>:air rates 0.105:2.63 and 0.088:2.204 g/min, respectively) led to different results. In this  
45  
46 261 case, lower rates promoted formation of C<sub>4</sub>A<sub>3</sub> $\bar{S}$  and C<sub>2</sub>S: the faster the gases passed over the  
47  
48 262 solid reactants the more this reaction was suppressed.  
49  
50  
51 263  
52  
53 264 Compositions with higher ye'elimite content, around 60%, could be achieved at temperatures as  
54  
55 265 low as 1200 °C (experiment 10 in Table 6); increasing the temperature to 1250 °C led to an  
56  
57 266 increase in both ye'elimite and belite contents (experiment 11 in Table 6).  
58  
59  
60  
61  
62  
63  
64  
65

1 267 The absence of ferrite in some clinkers could be attributed to the poorly crystalline ferrite, not  
2 268 'visible' by XRD, the possible inclusion of some iron, probably not exceeding a few wt. %, in  
3  
4 269 ye'elimite (Touzo, Scrivener & Glasser 2013), and the limitations of the XRD to detect small  
5  
6 270 amounts of phases.  
7

8 271

### 10 272 **3.5. Synthesis of clinkers using commercial grade reactants**

12 273 Table 7 and Table 8 show results of Rietveld analysis and thermodynamic modelling output,  
13  
14 274 respectively, of clinkers made with commercial grade raw materials (conditions shown in Table  
15  
16 275 4).

18 276 In the experiments with raw materials dilution of the SO<sub>2</sub> from SO<sub>2</sub>:air ratios of 1:25  
19  
20 277 (experiments 1 and 2 in Table 7) to 1:100 (experiments 3 and 4 in Table 7) led to a significant  
21  
22 278 increase in ye'elimite and belite. Also, the yield at 1300 °C is notably higher than at 1250 °C  
23  
24 279 (experiments 1-4 in Table 7).

26 280 These experiments indirectly show the effect of the presence of impurities in the raw materials  
27  
28 281 which affect stability and formation of the phases giving different results and different effect of  
29  
30 282 temperature and SO<sub>2</sub> partial pressure. The mineralogical evolution with time can be observed in  
31  
32 283 experiments 5-7 in Table 7: at 1300 °C and 1:100 SO<sub>2</sub>:air ratio, equilibrium seems to shift  
33  
34 284 towards formation of ye'elimite and belite with slow disappearance of gehlenite and calcium  
35  
36 285 sulfate.

38 286 According to the model predictions, the conditions used in experiments 2, 4 and 5-7 would lead  
39  
40 287 to the target compositions. The reasons why these were not achieved are likely due to kinetic  
41  
42 288 limitations, the ferrite not being 'visible' with XRD and possibly the cooling rate which may have  
43  
44 289 favoured formation of anhydrite and gehlenite as opposed to ye'elimite and belite. It must also  
45  
46 290 be noted that the model does not account for solid solutions (or liquid solutions) and can  
47  
48 291 therefore not predict the formation of entropy stabilised phases such as ye'elimite with iron  
49  
50 292 substitution or various aluminoferrite compositions.  
51

53 293

55 294 The formation of ternesite is predicted in four of the compositions (2, 3, 8 and 9 in Table 8) but  
56  
57 295 only detected experimentally in two (3 and 8 in Table 7). This can be understood by looking at  
58  
59 296 the temperatures and partial pressures which were used. Comparing experiments 2 and 3 from  
60

1 297 Table 4, both were carried out at SO<sub>2</sub>:air 1:100, but at different temperature. While in the  
2 298 experiment at 1250 °C ternesite could be seen, 1300 °C seems to be too high for ternesite to  
3  
4 299 stabilise. In experiments 8 and 9 from Table 4, both performed at 1275 °C, the lower SO<sub>2</sub> partial  
5  
6 300 pressure, 1:100 SO<sub>2</sub>:air ratio, favoured formation and stabilisation of ternesite as opposed to  
7  
8 301 1:50. Even though under ideal conditions ternesite would form in all cases, in reality too high  
9  
10 302 temperatures and too high partial pressures make it more difficult for it to be stabilised.

11  
12 303

#### 13 304 **4. Discussion**

14 305 At present, designing and implementing an “optimum” C $\bar{S}$ A clinker is arguably more difficult than  
15  
16 306 producing a PC clinker. Firstly, we do not at present know the “optimum” clinker mineralogy.  
17  
18 307 Should ternesite be present, and if so how much? Can we control the polymorphism of belite so  
19  
20 308 as to reproduce a reactive clinker with fast strength gain? And how are the economics of the  
21  
22 309 raw materials associated with the clinker mineralogy? How do the clinker phases react with  
23  
24 310 water and with each other to produce dense and durable matrices? Many questions remain  
25  
26 311 unanswered.

27  
28 312 But another complication arises: the presence of an important sulfur cycle in the course of  
29  
30 313 clinkering which can affect mineralogy. These dependencies, weak for PC cements, become  
31  
32 314 crucial in making C $\bar{S}$ A cement. The concept of using a reactive atmosphere to facilitate reaction  
33  
34 315 kinetics and control the quantitative clinker mineralogy is crucial but has not been well explored  
35  
36 316 in respect of C $\bar{S}$ A cement clinkering.

37  
38 317 It is known that gas-solid reactions are important to a range of problems, as for example, in  
39  
40 318 Portland cement clinkering, where the cycle of alkali circulation via the vapour phase may lead  
41  
42 319 to condensation in cooler zones of (K, Na) sulfates on the clinker and these in turn, affect early  
43  
44 320 hydration and set. However, the main oxide components of Portland cement are relatively  
45  
46 321 involatile and the vapour phase composition relatively unimportant to the circulation of the main  
47  
48 322 oxides. But cycles involving transfer of sulfur species assume much greater importance in the  
49  
50 323 course of clinkering C $\bar{S}$ A formulations where they control mass and energy balances. Both  
51  
52 324 C<sub>4</sub>A $\bar{3}$ S and C<sub>5</sub>S $\bar{2}$ S have definite limits of thermodynamic stability which need to be formulated in  
53  
54 325 terms of composition, temperatures and fugacities of both SO<sub>2</sub> and O<sub>2</sub>. Our approach to process  
55  
56 326 development and optimisation, combining thermodynamic calculation with experimentally -  
57  
58  
59  
60  
61  
62  
63  
64  
65

1 327 derived data, is being brought to maturity to guide and enhance clinker process development  
2 328 quantitatively to control clinker mineralogy.  
3  
4 329 Many commentators have expressed doubts that gas fugacities (which we equate with partial  
5  
6 330 pressures) can be controlled in a rotary kiln. While this may be true as a general case, special  
7  
8 331 circumstances arise in the formation of calcium sulfoaluminate clinkers which make control  
9  
10 332 relatively easy to achieve. For example, conventional kilns consume the oxygen components of  
11  
12 333 air with the result that the atmosphere in the burning zone has ca 1-4% free oxygen: typically an  
13  
14 334 order of magnitude less than air. If the oxygen pressure is allowed to drop below that range,  
15  
16 335 locally reducing conditions are generated which affect clinker quality: for example, ferric iron is  
17  
18 336 reduced to ferrous. Moreover, sulfur, if present, is chemically reduced to sulfide and CO  
19  
20 337 increasingly appears in exit gases. These processes are undesirable, so free oxygen is always  
21  
22 338 present in excess in combustion gas. On the other hand, if oxygen partial pressures are allowed  
23  
24 339 to rise, the thermal economy decreases as excess air is unnecessarily heated. Even if oxygen  
25  
26 340 enriched gas is used, the same set of restrictions apply. Broadly, we assume that these  
27  
28 341 considerations will also apply to C $\bar{S}$ A production. Thus, we assume that the oxygen partial  
29  
30 342 pressure will lie within a narrow range to optimise the clinkering process.  
31  
32 343 The sulfur species at elevated temperatures are dominated by SO<sub>2</sub> and its partial pressure is  
33  
34 344 fixed by temperature and by the sulfur content of the raw meal and fuel. As an approximation,  
35  
36 345 the vapour pressure of SO<sub>2</sub> in equilibrium with the clinker phases, e.g. anhydrite and ye'elimite,  
37  
38 346 can be used to fix the *minimum* numerical value of the partial pressures necessary to stabilise  
39  
40 347 these phases against evaporation. However, the actual pressure may significantly exceed that  
41  
42 348 minimum, as for example is likely to occur in the course of combusting sulfur- rich fuels, or when  
43  
44 349 elemental sulfur is injected into the kiln to supply part of the thermal energy.  
45  
46 350 Thus, we can distinguish three regimes in clinkering C $\bar{S}$ A compositions: (i) a regime with low  
47  
48 351 partial pressure of SO<sub>2</sub> in which the raw meal loses sulfur in order to saturate the kiln  
49  
50 352 atmosphere, (ii) a regime which is essentially neutral and no significant loss or gain of sulfur  
51  
52 353 occurs between solid and atmosphere and finally (iii), a regime mainly of higher SO<sub>2</sub> pressures  
53  
54 354 in which sulfur, effectively as "SO<sub>3</sub>", is transferred from the atmosphere to the solid. In order for  
55  
56 355 regime (iii) to operate, excess oxygen has to be present because, as noted, the transfer of sulfur  
57  
58  
59  
60  
61  
62  
63  
64  
65



1 356 from vapour to solid also involves an oxidation of the sulfur from S(IV) to S(VI). However, this  
2 357 condition is readily achieved by an excess of oxygen in the kiln atmosphere.  
3  
4 358 Despite the limitations of the experimental set-up, it was successfully proven that the transfer of  
5  
6 359 SO<sub>2</sub> and O<sub>2</sub> gas to the clinkering solids to form C $\bar{S}$ A clinkers occurs rapidly and efficiently under  
7  
8 360 normal operating conditions. It is also shown that clinkering temperatures tend to fall within a  
9  
10 361 narrow range. At temperatures below  $\approx 1230$  °C, reaction kinetics are too slow to achieve  
11  
12 362 complete reaction in the normal residence time in the hot zone, ca 20-60 minutes. On the other  
13  
14 363 hand, if it is desired to produce ternesite, which decomposes above an estimated 1298 °C (Gutt,  
15  
16 364 Smith 1967), clinkering temperatures cannot exceed this limit and the sulfur pressures need to  
17  
18 365 be maintained within limits determined by Hanein, et al (Hanein et al. 2017). If the limits are  
19  
20 366 observed, ternesite rich clinkers can be made in a single stage operation. However, ternesite  
21  
22 367 can only be considered as a desirable clinker mineral if, in clinker, its reactions with other  
23  
24 368 minerals and water leads to rapid strength gain: at present, this is not fully assured.  
25  
26 369 Ye'elimite containing clinkers have similar restrictive ranges where kinetics and equilibrium  
27  
28 370 allow it to form stably, but these limits are in general somewhat less restrictive than those of  
29  
30 371 ternesite. Above  $\approx 1320$  °C extensive melting occurs, so, depending on the target mineralogy,  
31  
32 372 clinkering temperatures will also lie in a narrow band between about 1250 and 1320 °C. The  
33  
34 373 other key variable, the partial pressure of SO<sub>2</sub>, greatly affects the mineralogy of the clinkers: at a  
35  
36 374 given temperature (around 1250-1300) a threshold in SO<sub>2</sub> partial pressure exists above which  
37  
38 375 C $\bar{S}$  and C<sub>2</sub>AS are more favourable to form than C<sub>4</sub>A<sub>3</sub>S $\bar{S}$  and C<sub>2</sub>S.  
39  
40 376 What is under less good control are the rates of sulfur transfer and their relation to the state or  
41  
42 377 condition of the gas- solid surface available for exchange. These are functions of, amongst  
43  
44 378 other factors, kiln size, gas flow rates and countercurrent solid flow rates, as well as total mass  
45  
46 379 of transferrable components. As such these factors are probably specific to specific equipment  
47  
48 380 and are not readily calculated without process data.  
49  
50 381 In this way, by combining technical and thermodynamic limits, it is possible to control the kiln  
51  
52 382 atmosphere simply by controlling the sulfur content of the fuel and raw mix and ensuring an  
53  
54 383 excess of oxygen.  
55  
56  
57  
58  
59  
60  
61  
62  
63  
64  
65

1 384 The knowledge gained from these experiments and calculations, that is, the influence of  
2 385 temperature and partial pressures of the gaseous components informed the pilot plants trials at  
3  
4 386 Ibutec, Weimar, Germany, reported in (Hanein et al. 2016).  
5  
6 387 Another important aspect of this work, controlling the polymorphism and reactivity of belite, is  
7  
8 388 still work in progress (Elhoweris, Galan & Glasser 2017). And, of course, hydration studies are  
9  
10 389 needed to determine the properties of the resulting binders at all ages. The correlation of clinker  
11  
12 390 mineralogy with cementing properties is under investigation (Jen et al. 2017).  
13

14 391

## 16 392 **5. Conclusions**

18 393 Experiments show that SO<sub>2</sub> and oxygen in the vapour are readily transferred to calcium  
19  
20 394 aluminates and silicates thereby combining much of the sulfur. Understanding the physical  
21  
22 395 chemistry of the process enables control over clinker phase composition and avoids production  
23  
24 396 of free lime, arising from decomposition of anhydrite and aluminates. The method emphasises  
25  
26 397 mass gains as opposed to more usual mass losses, which give greater freedom to design C $\bar{S}$ A  
27  
28 398 clinkers with optimised properties and utilise sulfur containing fuel whose heat of combustion  
29  
30 399 enables decrease consumption of hydrocarbon fuel and lowered CO<sub>2</sub> emissions.

32 400 Thermodynamic modelling has proven to be an invaluable tool with which to simulate, evaluate  
33  
34 401 and optimise novel cement compositions.  
35

36 402

## 38 403 **Acknowledgements**

40 404 The authors gratefully acknowledge the financial support provided by the Gulf Organization for  
41  
42 405 Research and Development (GORD), Qatar through University of Aberdeen research grant  
43  
44 406 number ENG016RGG11757.  
45

46 407

## 48 408 **References**

50 409 Bale, C.W., Chartrand, P., Degterov, S.A., Eriksson, G., Hack, K., Ben Mahfoud, R., Melançon,  
51  
52 410 J., Pelton, A.D. & Petersen, S. 2002, "FactSage thermochemical software and databases",  
53  
54 411 *Calphad: Computer Coupling of Phase Diagrams and Thermochemistry*, vol. 26, no. 2, pp. 189-  
55  
56 412 228.  
57  
58  
59  
60  
61  
62  
63  
64  
65

- 1 413 Barry, T.I. & Glasser, F.P. 2000, "Calculations of Portland cement clinkering reactions",  
2 414 *Advances in Cement Research*, vol. 12, no. 1, pp. 19-28.  
3  
4 415 Colville, A.A. & Geller, S. 1971, "The crystal structure of brownmillerite,  $\text{Ca}_2\text{FeAlO}_5$ ", *Acta*  
5 416 *Crystallographica Section B*, pp. 2311.  
6  
7 417 Cuesta, A., De La Torre, A.G., Losilla, E.R., Peterson, V.K., Rejmak, P., Ayuela, A., Frontera, C.  
8 418 & Aranda, M.A.G. 2013, "Structure, atomistic simulations, and phase transition of stoichiometric  
9 419 yeelimite", *Chemistry of Materials*, vol. 25, no. 9, pp. 1680-1687.  
10  
11 420 Cuesta, A., De La Torre, A.G., Losilla, E.R., Santacruz, I. & Aranda, M.A.G. 2014, "Pseudocubic  
12 421 crystal structure and phase transition in doped ye'elimite", *Crystal Growth and Design*, vol. 14,  
13 422 no. 10, pp. 5158-5163.  
14  
15 423 Davies, R.H., Dinsdale, A.T., Gisby, J.A., Robinson, J.A.J. & Martin, S.M. 2002, "MTDATA -  
16 424 Thermodynamic and phase equilibrium software from the national physical laboratory",  
17 425 *Calphad: Computer Coupling of Phase Diagrams and Thermochemistry*, vol. 26, no. 2, pp. 229-  
18 426 271.  
19  
20 427 Dollase, W.A. 1986, "Correction of intensities of preferred orientation in powder diffractometry:  
21 428 application of the March-model", *Journal of Applied Crystallography*, vol. 19, no. pt 4, pp. 267-  
22 429 272.  
23  
24 430 Elhoweris, A., Galan, I. & Glasser, F.P. 2017, "Stabilisation of belite polymorphs", *unpublished*.  
25  
26 431 Finger, L.W., Cox, D.E. & Jephcoat, A.P. 1994, "Correction for powder diffraction peak  
27 432 asymmetry due to axial divergence", *Journal of Applied Crystallography*, vol. 27, no. pt 6, pp.  
28 433 892-900.  
29  
30 434 Galan, I., Glasser, F.P., Elhoweris, A., Tully, S. & Murdoch, A. 2014, "Novel process for Calcium  
31 435 Sulfoaluminate Production", 34th Cement and Concrete Science Conference (CCSC) 2014.  
32  
33 436 Galan, I., Hanein, T., Elhoweris, A., Bannerman, M.N. & Glasser, F.P. 2017, "Phase  
34 437 compatibility in the system  $\text{CaO-SiO}_2\text{-Al}_2\text{O}_3\text{-SO}_3\text{-Fe}_2\text{O}_3$  and the effect of partial pressure on  
35 438 phase stability", *Industrial & Engineering Chemistry Research*, vol. 56, pp. 2341-2349.  
36  
37 439 Gartner, E. 2004, "Industrially interesting approaches to "low-CO<sub>2</sub>" cements", *Cement and*  
38 440 *Concrete Research*, vol. 34, no. 9, pp. 1489-1498.  
39  
40  
41  
42  
43  
44  
45  
46  
47  
48  
49  
50  
51  
52  
53  
54  
55  
56  
57  
58  
59  
60  
61  
62  
63  
64  
65

1  
2  
3  
4  
5  
6  
7  
8  
9  
10  
11  
12  
13  
14  
15  
16  
17  
18  
19  
20  
21  
22  
23  
24  
25  
26  
27  
28  
29  
30  
31  
32  
33  
34  
35  
36  
37  
38  
39  
40  
41  
42  
43  
44  
45  
46  
47  
48  
49  
50  
51  
52  
53  
54  
55  
56  
57  
58  
59  
60  
61  
62  
63  
64  
65

441 Gartner, E. & Hirao, H. 2015, "A review of alternative approaches to the reduction of CO<sub>2</sub>  
442 emissions associated with the manufacture of the binder phase in concrete", *Cement and*  
443 *Concrete Research*, vol. 78, pp. 126-142.

444 Gartner, E.M. & MacPhee, D.E. 2011, "A physico-chemical basis for novel cementitious  
445 binders", *Cement and Concrete Research*, vol. 41, no. 7, pp. 736-749.

446 Gutt, W. & Smith, M.A. 1967, "Studies of the Sub-system CaO-CaO.SiO<sub>2</sub>-CaSO<sub>4</sub>", *Transactions*  
447 *of the British Ceramic Society*, vol. 66.

448 Hanein, T., Elhoweris, A., Galan, I., Glasser, F.P. & Bannerman, M. 2015, "Thermodynamic  
449 data of ye'elemite (C<sub>4</sub>A<sub>3</sub>S̄) for cement clinker equilibrium calculations", 35th Cement and  
450 Concrete Science Conference 2015.

451 Hanein, T., Galan, I., Elhoweris, A., Khare, S., Skalamprinos, S., Jen, G., Whittaker, M., Imbabi,  
452 M.S., Glasser, F.P. & Bannerman, M.N. 2016, "Production of belite calcium sulfoaluminate  
453 cement using sulfur as a fuel and as a source of clinker sulfur trioxide: pilot kiln trial", *Advances*  
454 *in Cement Research*, vol. 28, no. 10, pp. 643-653.

455 Hanein, T., Galan, I., Glasser, F.P., Skalamprinos, S., Elhoweris, A., Imbabi, M.S. &  
456 Bannerman, M.N. 2017, "Stability of ternesite and the production at scale of ternesite-based  
457 clinkers", *Cement and Concrete Research* vol. 98 pp. 91-100.

458 Hanein, T., Glasser, F.P. & Bannerman, M. 2015, "Thermodynamics of Portland cement  
459 clinkering", 14th International Congress on the Chemistry of Cement (ICCC), 2015.

460 Hanein, T., Imbabi, M.S., Glasser, F.P. & Bannerman, M.N. 2016, "Lowering the carbon  
461 footprint and energy consumption of cement production: A novel calcium sulfoaluminate cement  
462 production process", *1st International Conference on Grand Challenges in Construction*  
463 *Materials*.

464 Hökfors, B., Boström, D., Viggh, E. & Backman, R. 2015, "On the phase chemistry of Portland  
465 cement clinker", *Advances in Cement Research*, vol. 27, no. 1, pp. 50-60.

466 Hökfors, B., Eriksson, M. & Viggh, E. 2014, "Modelling the cement process and cement clinker  
467 quality", *Advances in Cement Research*, vol. 26, no. 6, pp. 311-318.

468 Hörkner, W. & Müller-Buschbaum, H. 1976, "Zur kristallstruktur von CaAl<sub>2</sub>O<sub>4</sub>", *Journal of*  
469 *Inorganic and Nuclear Chemistry*, vol. 38, no. 5, pp. 983-984.

- 1 470 Idrissi, M., Diouri, A., Damidot, D., Greneche, J.M., Talbi, M.A. & Taibi, M. 2010,  
2 471 "Characterisation of iron inclusion during the formation of calcium sulfoaluminate phase",  
3  
4 472 *Cement and Concrete Research*, vol. 40, no. 8, pp. 1314-1319.  
5  
6 473 Irran, E., Tillmanns, E. & Hentschel, G. 1997, "Ternesite,  $\text{Ca}_5(\text{SiO}_4)_2\text{SO}_4$ , a new mineral from the  
7  
8 474 Ettringer Bellerberg/Eifel, Germany", *Mineralogy and Petrology*, vol. 60, no. 1-2, pp. 121-132.  
9  
10 475 Jen, G., Skalamprinos, S., Whittaker, M., Galan, I., Imbabi, M.S. & Glasser, F.P. 2017, "The  
11  
12 476 impact of intrinsic anhydrite in an experimental calcium sulfoaluminate cement from a novel,  
13  
14 477 carbon-minimized production process", *Materials and Structures*, vol. 50:144.  
15  
16 478 Juenger, M.C.G., Winnefeld, F., Provis, J.L. & Ideker, J.H. 2011, "Advances in alternative  
17  
18 479 cementitious binders", *Cement and Concrete Research*, vol. 41, no. 12, pp. 1232-1243.  
19  
20 480 Kirfel, A. & Will, G. 1980, "Charge density in anhydrite,  $\text{CaSO}_4$ , from X-ray and neutron  
21  
22 481 diffraction measurements", *Acta Crystallographica.*, vol. 36, no. 12, pp. 2881-2890.  
23  
24 482 Larson, A.C. & Von Dreele, R.B. 2004, "General structure analysis system (GSAS)", *Los*  
25  
26 483 *Alamos Laboratory, Rep.No.LA-UR*, vol. 86.  
27  
28 484 Louisnathan, S.J. 1971, "Refinement of the crystal structure of a natural gehlenite,  
29  
30 485  $\text{Ca}_2\text{Al}(\text{Al},\text{Si})_2\text{O}_7$ ", *Canadian Mineralogist*, vol. 10, pp. 822-837.  
31  
32 486 Mumme, W.G., Hill, R.J., Bushnell-Wye, G. & Segnit, E.R. 1995, "Rietveld crystal structure  
33  
34 487 refinements, crystal chemistry and calculated powder diffraction data for the polymorphs of  
35  
36 488 dicalcium silicate and related phases", *Neues Jahrbuch fuer Mineralogie - Abhandlungen*, vol.  
37  
38 489 169, no. 1, pp. 35.  
39  
40 490 Pliego-Cuervo, Y.B. & Glasser, F.P. 1978, "Role of sulphates in cement clinkering: The calcium  
41  
42 491 silicosulphate phase", *Cement and Concrete Research*, vol. 8, no. 4, pp. 455-459.  
43  
44 492 Roine, A. 2002, *HSC Chemistry 5.11*.  
45  
46 493 Sasaki, S., Prewitt, C.T., Bass, J.D. & Schulze, W.A. 1987, "Orthorhombic perovskite  $\text{CaTiO}_3$   
47  
48 494 and  $\text{CdTiO}_3$ : Structure and space group", *Acta Crystallographica, Sect.C*, vol. 43, pp. 1668-  
49  
50 495 1674.  
51  
52 496 Thompson, P., Cox, D.E. & Hastings, J.B. 1987, "Rietveld refinement of Debye-Scherrer  
53  
54 497 synchrotron X-ray data from  $\text{Al}_2\text{O}_3$ ", *Journal of Applied Crystallography*, vol. 20, pp. 79-83.  
55  
56  
57  
58  
59  
60  
61  
62  
63  
64  
65

1 498 Touzo, B., Scrivener, K.L. & Glasser, F.P. 2013, "Phase compositions and equilibria in the CaO-  
2 499 Al<sub>2</sub>O<sub>3</sub>-Fe<sub>2</sub>O<sub>3</sub>-SO<sub>3</sub> system, for assemblages containing ye'elimite and ferrite Ca<sub>2</sub>(Al,Fe)O<sub>5</sub>",  
3  
4 500 *Cement and Concrete Research*, vol. 54, pp. 77-86.  
5

6 501

7 502

8 503

9 504

10 **505 Figure captions**

11 506 Figure 1. Furnace used for the experiments where sulfur was transferred from the gas to the  
12 507 solid phase. The entire unit is housed in a ventilated enclosure 2400 mm width x 640 mm depth.

13 508 Note the red bar which is an edge of the sliding glass screen shown here in its open position.

14 509 Figure 2. Synthesis of ye'elimite from CaCO<sub>3</sub> and Al<sub>2</sub>O<sub>3</sub> in an atmosphere of SO<sub>2</sub>+air (ratio  
15 510 SO<sub>2</sub>:air of 1:2.5) at 1220 °C. Result after 30 minutes reaction.

16 511 Figure 3. Synthesis of ye'elimite from CaCO<sub>3</sub> and Al<sub>2</sub>O<sub>3</sub> in an atmosphere of SO<sub>2</sub>+air (ratio  
17 512 SO<sub>2</sub>:air of 1:25) at 1220 °C for 60 minutes.

18 513 Figure 4. Attempt to synthesize calcium sulfosilicate in an atmosphere of SO<sub>2</sub>+air (ratio SO<sub>2</sub>:air  
19 514 of 1:2.5) at 1220 °C for 60 minutes.

20 515 Figure 5. Formation of calcium sulfosilicate from C<sub>2</sub>S and C $\bar{S}$  in an atmosphere of SO<sub>2</sub>+air (ratio  
21 516 SO<sub>2</sub>:air of 1:25) at 1075 °C for 60 minutes.

22 517 Figure 6. Pellets with target composition 1 (Table 2) after firing at 1300 °C for 30 minutes under  
23 518 SO<sub>2</sub>+air atmosphere (ratio SO<sub>2</sub>:air of 1:2.5). Pellets are 13 mm diameter.

24 519 Figure 7. Pellets with target composition 2 (Table 2) after firing at 1300 °C for 30 minutes under  
25 520 SO<sub>2</sub>+air atmosphere (ratio SO<sub>2</sub>:air of 1:2.5). Pellets are 13 mm diameter.

26 521

27 522

28 **523 Table captions**

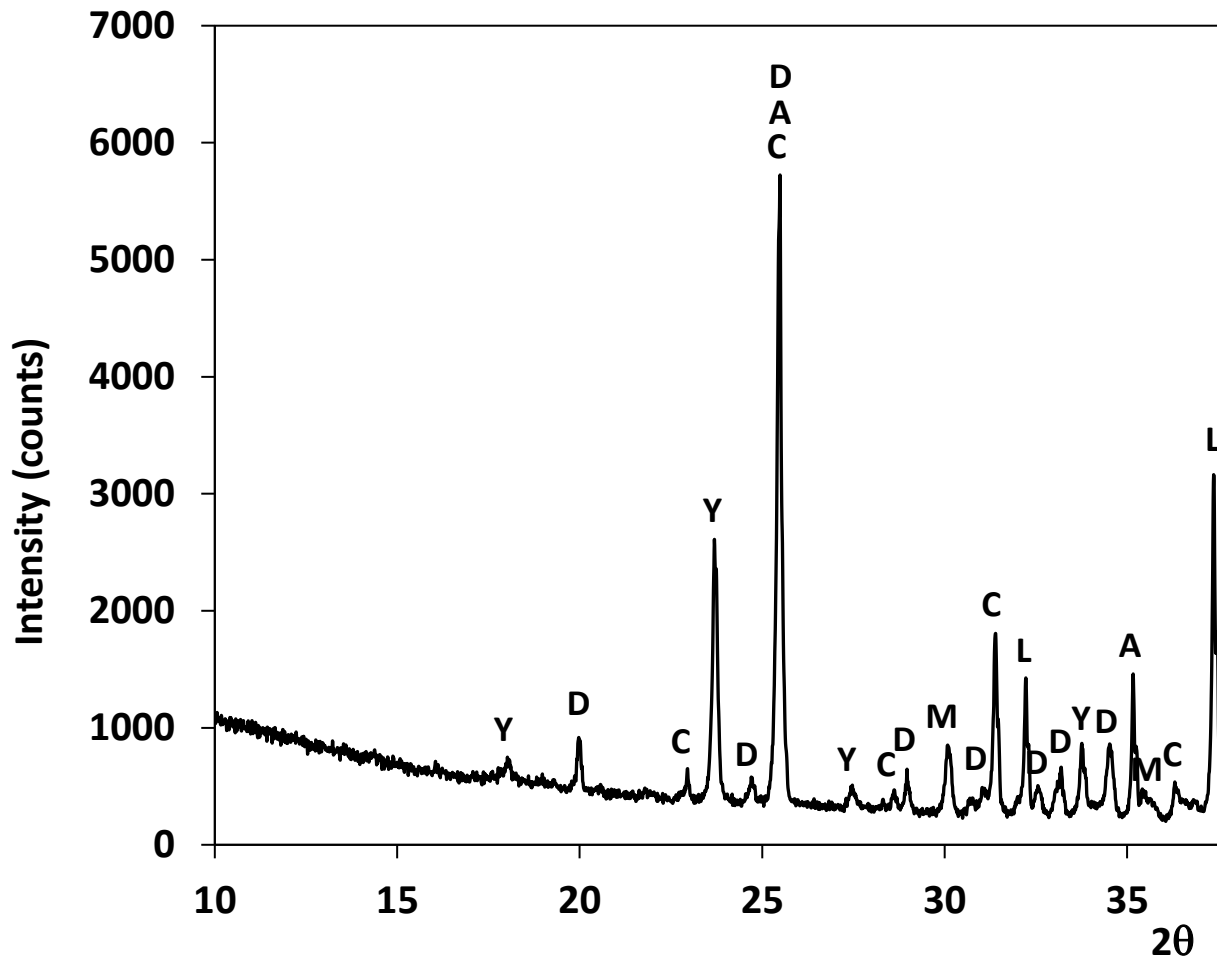
29 524 Table 1. Oxide composition of raw materials used for the experiments. XRF measurements of  
30 525 bauxite and clay were performed at Edinburgh University at the School of Geosciences. Oxide  
31 526 composition of limestone was provided by the supplier (Samin).  
32  
33  
34  
35  
36  
37  
38  
39  
40  
41  
42  
43  
44  
45  
46  
47  
48  
49  
50  
51  
52  
53  
54  
55  
56  
57  
58  
59  
60  
61  
62  
63  
64  
65

1 527 Table 2. Experimental conditions used for clinkers made with mixes of CaCO<sub>3</sub>, SiO<sub>2</sub>, Al<sub>2</sub>O<sub>3</sub> and  
2  
3 528 Fe<sub>2</sub>O<sub>3</sub>.  
4  
5 529 Table 3. Experimental conditions used for clinkers made with mixes of CaCO<sub>3</sub>, SiO<sub>2</sub>, Al<sub>2</sub>O<sub>3</sub>,  
6  
7 530 Fe<sub>2</sub>O<sub>3</sub> and CaSO<sub>4</sub>.  
8  
9 531 Table 4. Experimental conditions used for clinkers made with commercial grade raw materials.  
10  
11 532 Table 5. Rietveld analysis results of clinkers synthesized from laboratory grades of CaCO<sub>3</sub>,  
12  
13 533 SiO<sub>2</sub>, Al<sub>2</sub>O<sub>3</sub> and Fe<sub>2</sub>O<sub>3</sub>: experimental conditions shown in Table 2. Note the polymorphs of  
14  
15 534 C<sub>4</sub>A<sub>3</sub> $\bar{S}$  and C<sub>2</sub>S are included in the corresponding boxes. O and C stand for orthorhombic and  
16  
17 535 cubic ye'elimite, and  $\alpha'$ ,  $\beta$  and  $\gamma$  are the three polymorphs of C<sub>2</sub>S. wRp stands for weighted-  
18  
19 536 profile R factor.  
20  
21 537 Table 6. Rietveld analysis results of clinkers synthesized from laboratory grades of CaCO<sub>3</sub>,  
22  
23 538 SiO<sub>2</sub>, Al<sub>2</sub>O<sub>3</sub>, Fe<sub>2</sub>O<sub>3</sub> and CaSO<sub>4</sub>: experimental conditions shown in Table 3. Note the polymorphs  
24  
25 539 of C<sub>4</sub>A<sub>3</sub> $\bar{S}$ , orthorhombic (O) and cubic (C), are included in the corresponding box. All C<sub>2</sub>S formed  
26  
27 540 in these experiments was  $\beta$ -C<sub>2</sub>S.  
28  
29 541 Table 7. Rietveld analysis results of clinkers synthesized from commercial grade raw materials  
30  
31 542 clay, bauxite and limestone: experimental conditions shown in Table 4. Note the polymorphs of  
32  
33 543 C<sub>4</sub>A<sub>3</sub> $\bar{S}$  and C<sub>2</sub>S are included in the corresponding boxes. O and C stand for orthorhombic and  
34  
35 544 cubic ye'elimite, and  $\alpha'$  and  $\beta$  for the polymorphs of C<sub>2</sub>S.  
36  
37 545 Table 8. Model predictions for the clinker compositions made with commercial grade raw  
38  
39 546 materials: clay, bauxite and limestone. Temperature and gas atmosphere used for the  
40  
41 547 simulations are detailed in Table 4.  
42  
43 548  
44  
45 549  
46  
47 550  
48  
49  
50  
51  
52  
53  
54  
55  
56  
57  
58  
59  
60  
61  
62  
63  
64  
65

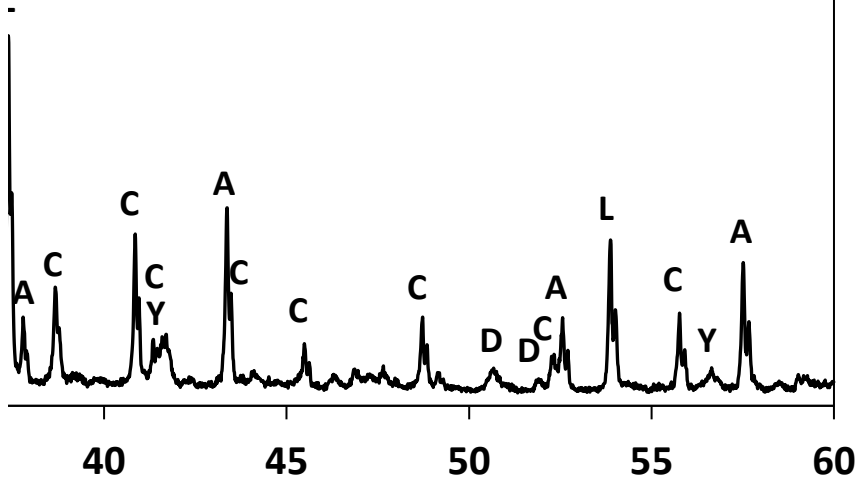




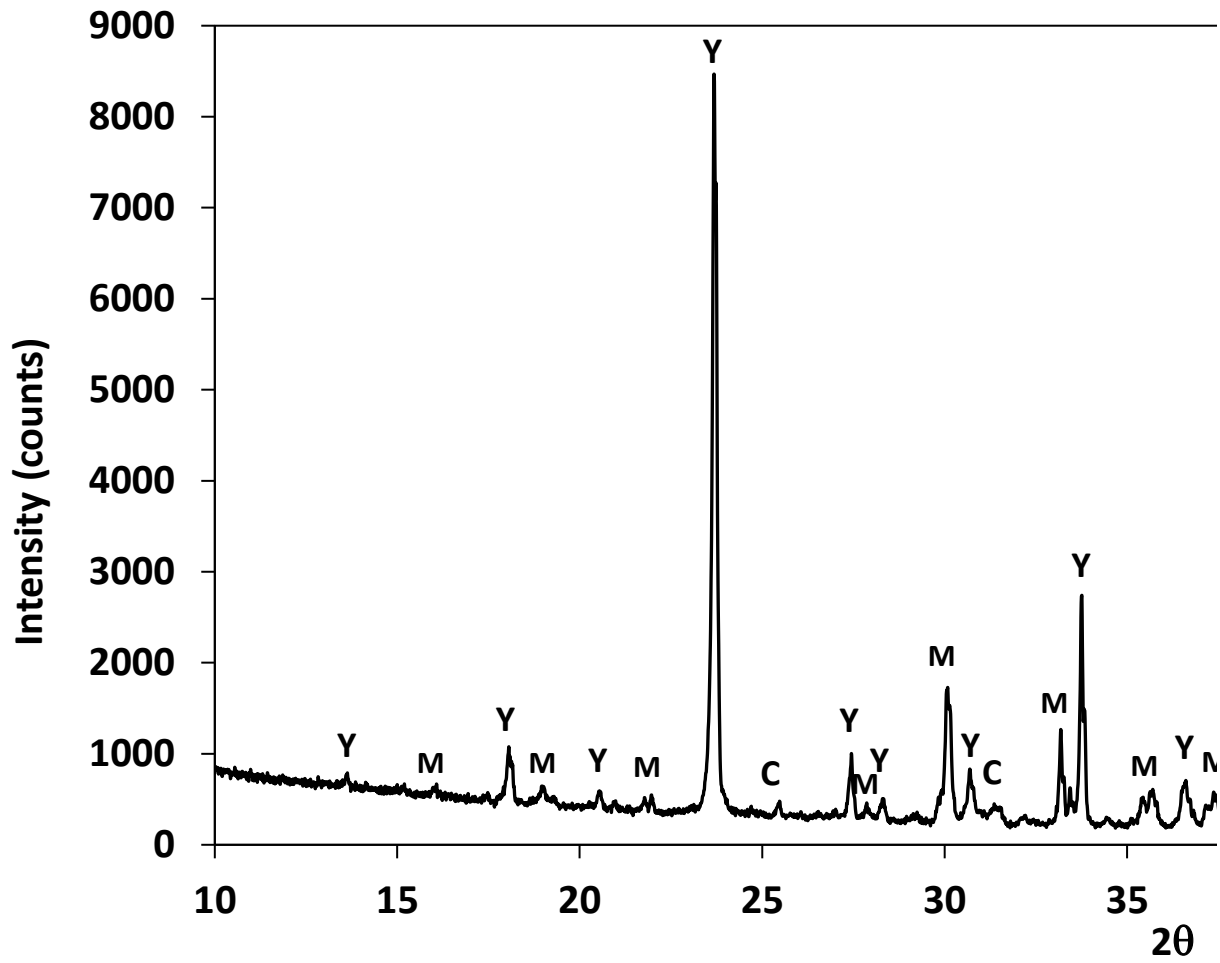
Figure



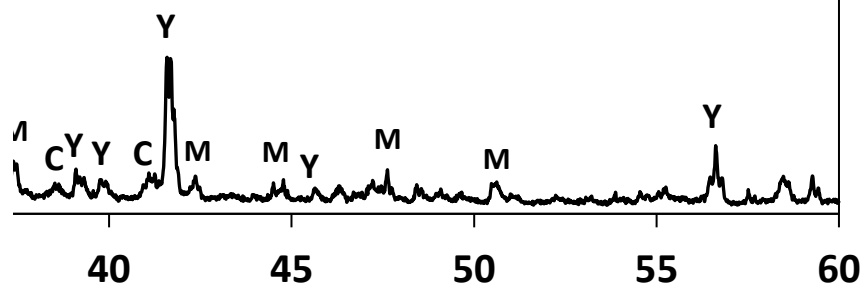
Y:  $C_4A_3S$   
M: CA  
C:  $C\ddot{S}$   
D:  $CA_2$   
L: CaO  
A:  $Al_2O_3$



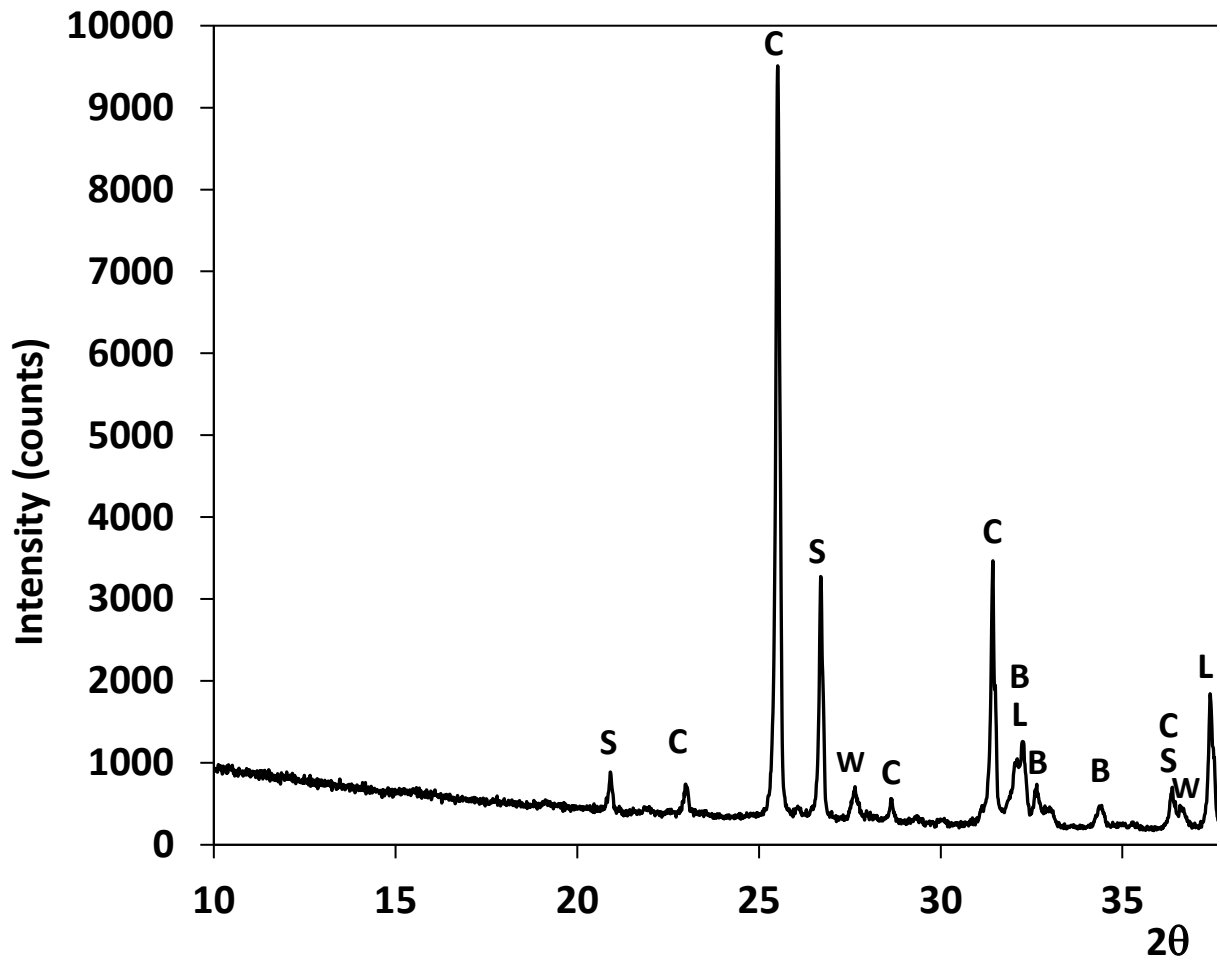
Figure



Y: C<sub>4</sub>A<sub>3</sub>S  
M: CA  
C: C<sub>2</sub>S



Figure



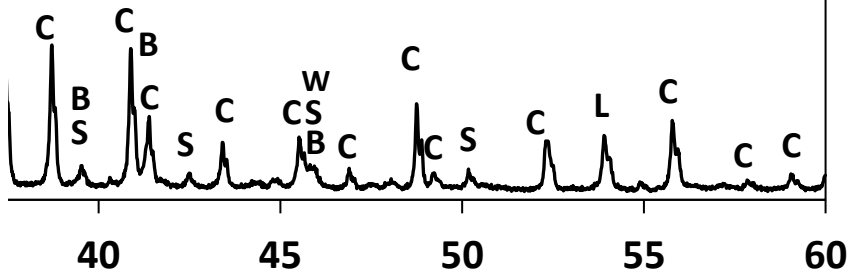
B: C<sub>2</sub>S

S: SiO<sub>2</sub>

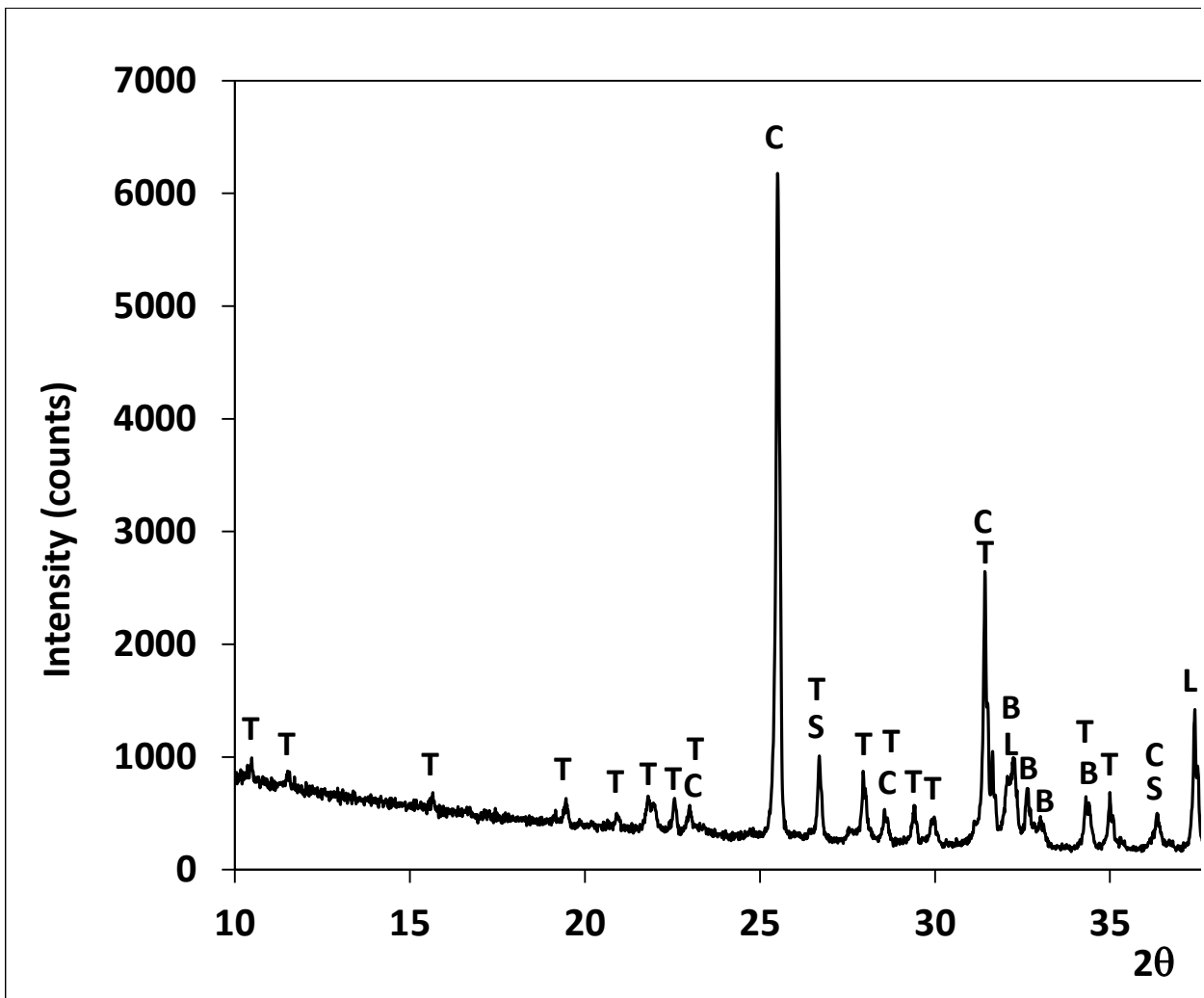
C: C $\bar{S}$

L: CaO

W: CS



Figure



B: C<sub>2</sub>S

S: SiO<sub>2</sub>

C: C $\ddot{S}$

L: CaO

T: C<sub>5</sub>S<sub>2</sub> $\ddot{S}$

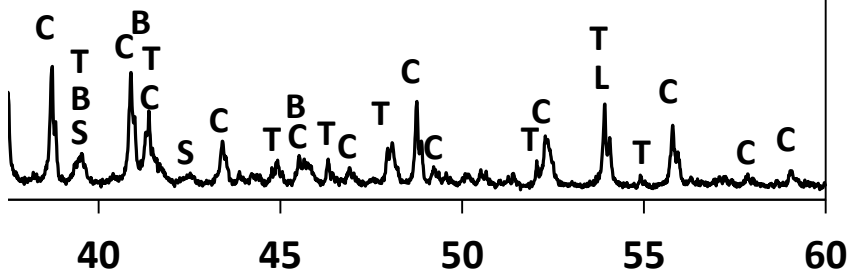








Table 1. Oxide composition of raw materials used for the experiments. XRF measurements of bauxite and clay were performed at Edinburgh University at the School of Geosciences. Oxide composition of limestone was provided by the supplier (Samin).

% Oxides	Bauxite	Clay	Limestone
SiO <sub>2</sub>	11.52	39.24	0.1
Al <sub>2</sub> O <sub>3</sub>	69.32	38.18	0.00
Fe <sub>2</sub> O <sub>3</sub>	1.21	5.98	0.009
MgO	0.00	0.06	0.26
CaO	0.16	0.87	55.70
Na <sub>2</sub> O	0.00	0.00	0.00
K <sub>2</sub> O	0.455	0.624	0.00
TiO <sub>2</sub>	3.409	1.773	0.00
MnO	0.000	0.001	0.00
P <sub>2</sub> O <sub>5</sub>	0.081	0.088	0.00
LOI	13.44	13.08	44.00

Table 2. Experimental conditions used for clinkers made with mixes of  $\text{CaCO}_3$ ,  $\text{SiO}_2$ ,  $\text{Al}_2\text{O}_3$  and  $\text{Fe}_2\text{O}_3$ .

	Target mineralogy (weight %)	Input (weight % solids)	Mass flow rates $\text{SO}_2$ :air (g/min)	Temperature ( $^{\circ}\text{C}$ )
1	60% $\text{C}_4\text{A}_3\text{S}$ 20% $\text{C}_2\text{S}$ 20% $\text{C}_6\text{A}_2\text{F}$	48.1% $\text{CaO}$ 7.6% $\text{SiO}_2$ 37.2% $\text{Al}_2\text{O}_3$ 7.1% $\text{Fe}_2\text{O}_3$	0.04:0.1 (1:2.5)	1300
2	40% $\text{C}_4\text{A}_3\text{S}$ 40% $\text{C}_2\text{S}$ 20% $\text{C}_6\text{A}_2\text{F}$	52.7% $\text{CaO}$ 14.7% $\text{SiO}_2$ 25.6% $\text{Al}_2\text{O}_3$ 6.9% $\text{Fe}_2\text{O}_3$	0.04:0.1 (1:2.5)	1300
3	20% $\text{C}_4\text{A}_3\text{S}$ 60% $\text{C}_2\text{S}$ 20% $\text{C}_6\text{A}_2\text{F}$	57.1% $\text{CaO}$ 21.5% $\text{SiO}_2$ 14.6% $\text{Al}_2\text{O}_3$ 6.8% $\text{Fe}_2\text{O}_3$	0.04:0.1 (1:2.5)	1300

Table 3. Experimental conditions used for clinkers made with mixes of  $\text{CaCO}_3$ ,  $\text{SiO}_2$ ,  $\text{Al}_2\text{O}_3$ ,  $\text{Fe}_2\text{O}_3$  and  $\text{CaSO}_4$ .

	Target mineralogy (weight %)	Input (weight %)	Mass flow rates $\text{SO}_2$ :air (g/min)	T (°C)
1			1.05:2.63 (1:2.5)	
2			0.105:2.63 (1:25)	
3		52.1% CaO	0.1:5 (1:50)	1280
4	30% $\text{C}_4\text{A}_3\text{S}$	20.9% $\text{SiO}_2$	0.04:4 (1:100)	
5	60% $\text{C}_2\text{S}$	6.7% $\text{CaSO}_4$	0.04:2 (1:50)	1230
6	10% $\text{C}_6\text{A}_2\text{F}$	18.0% $\text{Al}_2\text{O}_3$	0.04:1 (1:25)	1230
7		2.3% $\text{Fe}_2\text{O}_3$		1200
8			0.088:2.204 (1:25)	1250
9				1270
10		40.9% CaO		1200
	60% $\text{C}_4\text{A}_3\text{S}$	10.5% $\text{SiO}_2$		
11	30% $\text{C}_2\text{S}$	13.4% $\text{CaSO}_4$	0.088:2.204 (1:25)	
	10% $\text{C}_6\text{A}_2\text{F}$	33.0% $\text{Al}_2\text{O}_3$		1250
		2.3% $\text{Fe}_2\text{O}_3$		

Table 4. Experimental conditions used for clinkers made with commercial grade raw materials.

	Target mineralogy (weight %)	Input (weight %)	Flow rates SO <sub>2</sub> :air (g/min)	Temperature (°C)	Time (min)
1	36% C <sub>4</sub> A <sub>3</sub> S			1250	
2	32% C <sub>2</sub> S	12.2% bauxite	0.04:1 (1:25)	1300	120
3	9% C <sub>4</sub> AF	68.4% limestone		1250	
4	23% C <sub>5</sub> S	19.5% clay	0.04:4 (1:100)	1300	
5					120
6	34% C <sub>4</sub> A <sub>3</sub> S	6.6% bauxite		1300	60
7	42% C <sub>2</sub> S	67.3% limestone	0.04:4 (1:100)		30
8	11% C <sub>4</sub> AF	26.1% clay		1275	120
9	13% C <sub>5</sub> S		0.04:2 (1:50)		

Table 5. Rietveld analysis results of clinkers synthesized from laboratory grades of  $\text{CaCO}_3$ ,  $\text{SiO}_2$ ,  $\text{Al}_2\text{O}_3$  and  $\text{Fe}_2\text{O}_3$ : experimental conditions shown in Table 2. Note the polymorphs of  $\text{C}_4\text{A}_3\text{S}$  and  $\text{C}_2\text{S}$  are included in the corresponding boxes. O and C stand for orthorhombic and cubic ye'elinite, and  $\alpha'$ ,  $\beta$  and  $\gamma$  are the three polymorphs of  $\text{C}_2\text{S}$ . wRp stands for weighted- profile R factor.

	Target mineralogy (weight %)	Output mineralogy (weight %)								wRp (%)
		$\text{C}_4\text{A}_3\text{S}$	$\text{C}_2\text{S}$	$\text{C}_3\text{S}$	$\text{C}_2\text{AS}$	$\text{C}_4\text{AF}$	S	$\text{C}_3\text{A}$	$\text{C}_{12}\text{A}_7$	
1	60% $\text{C}_4\text{A}_3\text{S}$ 20% $\text{C}_2\text{S}$ 20% $\text{C}_6\text{A}_2\text{F}$	O 20 C 28	$\alpha'$ 1 $\beta$ 2	23	26	1				5.28
2	40% $\text{C}_4\text{A}_3\text{S}$ 40% $\text{C}_2\text{S}$ 20% $\text{C}_6\text{A}_2\text{F}$	O 15 C 23	$\alpha'$ 2 $\beta$ 19	18	21	1				4.99
3	20% $\text{C}_4\text{A}_3\text{S}$ 60% $\text{C}_2\text{S}$ 20% $\text{C}_6\text{A}_2\text{F}$	O 2	$\beta$ 25 $\gamma$ 18		1	28	4	20	1	5.48

Table 6. Rietveld analysis results of clinkers synthesized from laboratory grades of  $\text{CaCO}_3$ ,  $\text{SiO}_2$ ,  $\text{Al}_2\text{O}_3$ ,  $\text{Fe}_2\text{O}_3$  and  $\text{CaSO}_4$ : experimental conditions shown in Table 3. Note the polymorphs of  $\text{C}_4\text{A}_3\text{S}$ , orthorhombic (O) and cubic (C), are included in the corresponding box. All  $\text{C}_2\text{S}$  formed in these experiments was  $\beta\text{-C}_2\text{S}$ .

	Target mineralogy (weight %)	Output mineralogy (weight %)								wRp (%)	
		$\text{C}_4\text{A}_3\text{S}$	$\beta\text{-C}_2\text{S}$	C $\text{S}$	$\text{C}_2\text{AS}$	$\text{C}_5\text{S}_2\text{S}$	CA	$\text{C}_4\text{AF}$	C		S
1		O 1 C 4		57	38						5.68
2		O 17 C 12	33	16	22						5.57
3		O 19 C 13	37	12	19						4.72
4		O 15 C 19	33	11	21						5.74
5	30% $\text{C}_4\text{A}_3\text{S}$ 60% $\text{C}_2\text{S}$ 10% $\text{C}_6\text{A}_2\text{F}$	O 9 C 10	13	41	13	4	7	1		2	8.33+
6		O 24 C 11	35	12	5	2		4	4	2	5.23
7		O 23 C 8	21	24	4	8		3	6	4	6.00
8		O 15 C 14	32	21	14	4					5.89
9		O 27 C 16	40	13	5						5.70
10	60% $\text{C}_4\text{A}_3\text{S}$ 30% $\text{C}_2\text{S}$ 10% $\text{C}_6\text{A}_2\text{F}$	O 43 C 15	8	17	2	4	4	2	4		5.81
11		O 63	14	16	7						9.22



Table 7. Rietveld analysis results of clinkers synthesized from commercial grade raw materials clay, bauxite and limestone: experimental conditions shown in Table 4. Note the polymorphs of  $C_4A_3S$  and  $C_2S$  are included in the corresponding boxes. O and C stand for orthorhombic and cubic ye'elimite, and  $\alpha'$  and  $\beta$  for the polymorphs of  $C_2S$ .

	Target mineralogy (weight %)	Output mineralogy (weight %)					wRp (%)	
		$C_4A_3S$	$C_2S$	$C_3S$	$C_2AS$	CT		$C_3S_2S$
1		O 1 C 4		64	31	1		9.46
2	36% $C_4A_3S$ 32% $C_2S$	O 8 C 13	$\beta$ 4 $\alpha'$ 2	48	25		1	9.30
3	9% $C_4AF$ 23% $C_3S$	O 20 C 17	$\beta$ 11 $\alpha'$ 7	29	4	2	11	6.79
4		O 30 C 16	$\beta$ 23 $\alpha'$ 8	22		1	0	5.63
5		O 22 C 20	$\beta$ 28 $\alpha'$ 3	23		5		8.46
6		O 10 C 32	$\beta$ 23 $\alpha'$ 3	27	3	3		8.63
7	34% $C_4A_3S$ 42% $C_2S$ 11% $C_4AF$	O 13 C 23	$\beta$ 19 $\alpha'$ 2	32	9	1	2	6.93
8	12% $C_3S$	O 8 C 25	$\beta$ 9	27	11	1	18	6.60
9		O 1 C 1		59	39			10.62

Table 8. Model predictions for the clinker compositions made with commercial grade raw materials: clay, bauxite and limestone. Temperature and gas atmosphere used for the simulations are detailed in Table 4.

Model Output (weight %) using raw materials								
	C <sub>4</sub> A <sub>3</sub> S	C <sub>2</sub> S	C <sub>3</sub> S	C <sub>4</sub> AF	C <sub>5</sub> S <sub>2</sub> S	CT	CF (L)	MgO
1	38.7	-	12.8	-	44.5	1.6	2.2	0.2
2	37.2	32.4	23.5	5.0	-	1.6	-	0.2
3	37.2	-	10.7	5.0	45.2	1.6	-	0.2
4	37.2	32.4	23.5	5.0	-	1.6	-	0.2
5	35.6	42.0	14.0	6.6		1.5	-	0.3
6	35.6	42.0	14.0	6.6		1.5	-	0.3
7	35.6	42.0	14.0	6.6		1.5	-	0.3
8	35.6	6.4	-	6.6	49.6	1.5	-	0.3
9	35.6	6.4	-	6.6	49.6	1.5	-	0.3



## Journal Publishing Agreement

It is our policy to ask authors to assign the copyright of articles accepted for publication to the Publisher. Exceptions are possible for reasons of national rules or funding. Please tick the relevant options below.

In assigning copyright to us, you retain all proprietary rights including patent rights, and the right to make personal (non-commercial) use of the article, subject to acknowledgement of the journal as the original source of publication.

By signing this agreement, you are confirming that you have obtained permission from any co-authors and advised them of this copyright transfer. Kindly note that copyright transfer is not applicable to authors who are opting to publish their papers as Open Access. Open Access authors retain copyright of their published paper.

Please complete the form below and return an electronic copy to your ICE Publishing contact:  
(<http://www.icevirtuallibrary.com/info/submit>).

Journal name: ADVANCES IN CEMENT RESEARCH  
 Article title: ADVANCES IN CLINKERING TECHNOLOGY OF CALCIUM SULFOALUMINATE CEMENT  
 Manuscript reference number: ACR-D-17-00028  
 Authors: I. GALAN, A. ELHOUWERIS, T. HANEIN, M. BANWERMANN, F.P. GLASSER  
 Your name: ISABEL GALAN  
 Signature and date: [Signature] 28 April 2017

Please tick either one option from part A or one option from part B. Please complete part C.

### A. Copyright

- I hereby assign and transfer the copyright of this paper to Thomas Telford Ltd.
- British Crown Copyright: I hereby assign a non-exclusive licence to publish to Thomas Telford Ltd.
- I am a US Government employee: employed by (name of agency) .....
- I am subject to the national rules of (country) ..... and confirm that I meet their requirements for copyright transfer or reproduction (please delete as appropriate)

### B. Authors with open access funding requirements. Please specify the Creative Commons license version required.

- CC-BY (for full details click here [Creative Commons Attribution \(CC BY\) 4.0 International License](#))
- CC-BY-NC-ND (for full details click here [Creative Commons Attribution Non Commercial No-derivatives \(CC BY NC ND\) 4.0 International License](#))

### C. Please confirm that you have obtained permission from the original copyright holder. For ICE Publishing's copyright policy, please click [here](#). ICE Publishing is a signatory to the [STM Guidelines](#).

- I have obtained permission from the original copyright holder for the use of all subsidiary material included in this paper (E.g. for borrowed figures or tables).

To the editor and referees,

Enclosed is a manuscript to be considered for publication in "Advances in Cement Research", entitled 'Advances in clinkering technology of calcium sulfoaluminate cement'.

The manuscript describes a new process to produce cement. The main highlight of the process is the use of sulfur, in gas phase, as a raw material to produce calcium sulfoaluminate clinkers. The method presents important advantages in terms of CO<sub>2</sub> and energy savings. The experimental design to develop the new method is described. The experimental and thermodynamic modelling results presented here lead to the completion of pilot plant trials (published in ACR vol 28, 2016).

We appreciate your consideration and look forward to its publication.

Yours sincerely,

Isabel Galan, Ammar Elhoweris, Theodore Hanein, Marcus Bannerman, Fredrik P. Glasser